Contents list available at CBIORE journal website

International Journal of Renewable Energy Development

Journal homepage: https://ijred.cbiore.id

Research Article

An electro-thermal modeling of distribution transformer for hottest spot evaluation under photovoltaic-induced harmonics

Muhammad Haziq Mohd Wazir[a,b*], Dalila Mat Said[a,b], Norazliani Md Sapari[a,b], Mohamed Shahriman Mohamed Yunus[c], Zaris Izzati Mohd Yassin[d]

[a]*Centre of Electrical Energy Systems, Institute of Future Energy, Universiti Teknologi Malaysia, Skudai, Malaysia*

[b]*Faculty of Electrical Engineering, Universiti Teknologi Malaysia, Skudai, Malaysia*

[c]*Electrical Engineering Branch, Public Works Departments of Malaysia, Kuala Lumpur, Malaysia*

[d]*School of Engineering and Computing, Mila University,Nilai, Malaysia*

Abstract. Elevated winding insulation temperature, driven by harmonic distortions, is a key factor in transformer lifespan reduction. Conventional models often oversimplify the effect of combined current and voltage harmonics. This paper proposes an electro-thermal modeling approach, incorporating dual heat sources from core and winding domains, to enhance HST estimation in distribution transformers affected by photovoltaic-induced (PV)-induced harmonic losses. A sophisticated numerical approach, Finite Element Analysis (FEA), is employed using COMSOL Multiphysics software, with a 250-minute time-dependent study assessing thermal effects. The results, verified against a mathematical model approach based on IEEE C57.110-2018 guidance, demonstrate that higher levels of harmonics lead to a rapid increase in HST, accelerating the time to reach the aging factor temperature and consequently diminishing the transformer's operational lifespan. Specifically, the per-unit life of the transformer decreases from 0.219 in Case 1 to 0.154 in Case 2 and 0.027 in Case 3, while the aging acceleration factor increases from 4.310 to 5.683 and 21.7, respectively. The methods showed over 95% alignment with the mathematical modeling approach, confirming the model's precision in its predictive capability. The novelty of this study lies in its enhanced electro-thermal framework, which overcomes the limitations of conventional methods by integrating dual heat sources and providing a refined assessment of transformer aging under harmonic distortions. This advancement offers a more precise and computationally efficient approach for assessing transformer thermal stress under harmonic distortions.

Keywords: Distribution transformer, harmonics, hotspot temperature, photovoltaic systems, winding insulation.

Received: 24th Dec 2024; Revised: 27th Feb 2025; Accepted: 18th March 2025; Available online:25th March 2025

1. Introduction

The stability of an electrical distribution network critically depends on the condition of its distribution transformers. One major factor contributing to transformer failure is the elevation of its winding insulation temperature, exacerbated by the presence of harmonic distortions. Harmonic distortions have become increasingly significant with the widespread integration of renewable energy systems, particularly photovoltaic (PV) systems (Ackermann *et al.*, 2001; Hamza *et al.*, 2021; Hossain *et al.*, 2023; Panigrahi *et al.*, 2020). Harmonics, which are electrical distortions at multiple of the fundamental frequency, can originate from various non-linear loads in distribution systems. With the introduction of PV systems and inverters, these harmonics are becoming more pronounced. This interaction may lead to the amplification of certain harmonic frequencies, creating a distinct harmonic spectrum within the transformer (Hajipour *et al.* 2017; Ruiz *et al.* 2021; Yuan *et al*, 2023). The intermittent nature of solar energy generation, specifically from PV systems, introduces voltage and current harmonics, that yield greater core and winding losses, leading to higher temperature rises (Uçar *et al.* 2017). Studies have shown that the harmonic current content produced by transformers can increase due to direct current (DC) injection from PV inverters (Fortes *et al.* 2020). In one such study, a 45 kVA three-phase five-legged transformer demonstrated that harmonic current propagation was higher when the inverter operated at 20% of its nominal power. This highlights the impact of PV inverter operating conditions on harmonic distortions in transformers. The introduction of PV systems into distribution networks can also increase transformer load losses and potential failures, as demonstrated by Majeed & Nwulu, (2022), where the increased penetration of PV systems in a low-voltage radial distribution system elevated transformer load loss.

1.1 Related Works

Temperature is a critical in determining transformer performance and longevity (Abdali *et al.* 2024; AJ *et al.* 2018; El Batawy & Morsi, 2017; León-Martínez *et al.* 2023; Yang *et al.*, 2019). The winding insulation, as the most thermally vulnerable component, is designed to prevent the winding's HST from

* Corresponding author
Email: haziq@graduate.utm.my (M.H.M Wazir)

https://doi.org/10.61435/ijred.2025.60959
ISSN: 2252-4940/© 2025.The Author(s). Published by CBIORE

Table 1
Literature Overview

Author (Year)	System Configuration	Harmonics Consideration		Transformer Loss Evaluation				Heat Source		Lifetime Estimation	
	PV-Grid	Current	Voltage	Load Loss: Ohmic	Load Loss: Eddy current	Load Loss: Other Stray	No Load Loss: Core	Winding Domain	Core Domain	PU Life	FAA
Awadallah *et al.* (2016)	/	/	/					/		/	
Laoena *et al.* (2017)		/	/	/	/	/					
Dao *et al.* (2017)			/				/		/	/	
Taheri *et al.* (2019)	/							/	/	/	
Said *et al.* (2020)		/		/	/			/			
Dawood *et al.* (2021)			/				/		/		
Ruiz *et al.* (2021)	/		/				/			/	
Majeed *et al.* (2022)	/	/			/						
Thango *et al.* (2022)	/	/		/	/	/		/		/	/
Mitra *et al.* (2023)	/	/			/			/			
Rajput *et al.* (2023)	/	/		/	/	/		/		/	
Proposed Method	/	/	/	/	/	/	/	/	/	/	/

exceeding a specific limit. Surpassing this limit accelerates insulation degradation, leading to reduced transformer life and premature failure. Factors such as harmonics, load variation, and other operational conditions contribute to temperature rise (Cazacu *et al.* 2018; Soleimani & Kezunovic, 2020). Effective temperature analysis is essential for managing aging, insulation health, and operational lifespan. Monitoring temperature, particularly under harmonic distortion, is crucial for health monitoring, predictive maintenance, and load management (Américo *et al.* 2024; Awadallah *et al.* 2015; Gorginpour *et al.* 2022; Lu *et al.* 2019). For instance, Awadallah *et al.* (2015), have attempted a lifetime estimation of a three-phase dry-type transformer. The authors quantified the amount of harmonic distortion caused by solar panel and its inverter using experimental approach. The worst loading scenario case caused increment on the winding HST which reduced 8.3% of its lifetime. The study has its limitation, where the impact of voltage harmonics towards the lifetime reduction is not considered. Another novel approach was proposed by Taheri *et al.*, (2019), who studied the thermal behavior of a 500 kVA oil-immersed transformer using a Thermal Radiation Model that incorporated solar radiation. This study demonstrated how solar radiation influences transformer oil temperature and, consequently, the loss of life due to increased temperatures. Thango & Bokoro, (2022) suggested modifying the IEEE loading guide standard of HST formulation to create a more detailed thermal model for predicting temperature rise under harmonic load conditions. On the other hand, Wan *et al.*, (2019) focused on the effect of harmonic distortion levels, reporting a dramatic temperature rise at a 40% harmonic distortion rate, where HST reached 102.7 K, exceeding the safe operational limit of 78 K. This study highlights the direct link between high harmonic content and the risk of thermal damage, emphasizing the need for regulatory measures to cap distortion levels. Chen *et al.* (2023) investigated converter transformers and observed differential effects of harmonic currents on winding temperatures. The study found that the grid-side winding experienced a 2.7°C increase in HST, while the valve-side winding saw a 1.6°C rise. These findings indicate that harmonic currents unevenly impact winding losses, necessitating targeted strategies for loss reduction in specific winding regions. Shaoxin *et al.* (2019) provided a contrasting perspective by calculating HST under controlled harmonic conditions. The study reported an HST of 73.4°C, which, while elevated, remained within safe operational limits. This finding suggests that transformers can tolerate certain levels of harmonic distortion without compromising safety, provided effective thermal management strategies are implemented. Liu *et al.* (2024) provided a detailed quantification of winding losses and HST in UHV converter transformers under high-frequency harmonic currents. The study revealed that winding losses increase exponentially with frequency, leading to substantial temperature rises. Moreover, the study validated its simulation accuracy, reporting a hotspot temperature error of just 0.58 K. These precise measurements underscore the reliability of advanced modeling approaches for predicting harmonic-induced thermal impacts.

Electro-thermal modeling methods, such as the Finite Element Analysis (FEA), have proven highly effective in modeling and analyzing the thermal behavior of transformers under various operating conditions. For instance, it was employed by Si *et al.*, (2020) to examine the impact of magnetic flux and eddy current losses on the HST of oil circulation transformers. This study revealed that leakage magnetic flux tends to concentrate at the core's contact points, leading to

increased hotspot temperatures and greater inner temperature difference within the coil. Similarly, FEA modeling was also applied by (Das & Chatterjee, 2017) in focusing on the flow rate and temperature distribution in oil-filled disc-type winding transformers, emphasizing the effect of cooling duct dimension on hotspot location and temperature. Xiao *et al.* (2022) utilized a thermal-fluid coupling model using FEM to study the temperature field distribution and hot spot temperature rise in oil-type transformers under rated operation and over-nameplate load conditions, primarily influenced by ohmic losses. However, the study does not specifically address the impact of harmonic towards transformer hotspot temperature. Said *et al.* (2020) employed FEA to analyze the effects of unbalanced harmonic loads, highlighting a substantial rise in HST when transitioning from a rated load to an unbalanced harmonic load. The study focused exclusively on eddy current losses generated by harmonic currents, where a single heat source generated from the eddy current harmonic loss is appointed in the transformer thermal model. However, the study could be improved by analyzing the concurrent impact of both current and voltage harmonics through the influence of PV systems on different harmonic losses generation.

1.2 Research Gap and Novelty

Recent research has extensively investigated the effect of harmonics on transformer performance, indicating their potential to worsen temperature increases due to higher eddy current losses and core saturation (Awadallah *et al.*, 2016; Dao & Phung, 2018). However, existing literature often separates the impact of current harmonics and voltage harmonics on the operational condition of the transformer, as portrayed in Table 1, leaving a significant gap in understanding their concurrent influence on both load and no-load losses. These losses are critical factors in determining a transformer's definitive temperature rise and overall operational health. While traditional methods provide foundational insights, they fail to meet the combined effects of harmonics on transformer performance, particularly, under the complex conditions introduced by renewable energy integration. This gap underscores the need for extensive examinations that consider the simultaneous impact of harmonics on both load and no-load conditions, which is essential for accurate transformer health and lifetime prediction. To address this gap, this study introduced a novel dual heat source approach that uniquely integrates the effect of both core and winding losses under harmonic distortions, a perspective that has not been comprehensively explored in prior research. Unlike conventional methods that treat core and winding losses separately (Abdali *et al.*, 2024; Said *et al.*, 2020), the proposed electro-thermal model, developed using FEA, captures the thermal interactions between the two heat sources. This integrated approach enables a more accurate estimation of the HST and provides a detailed understanding of the thermal stresses imposed on transformer insulation under harmonic-rich environments. The novelty of this work lies in its ability to bridge the gap between load and no-load loss analysis, offering a unified framework that captures the combined impact of harmonics on transformer performance. By leveraging this advanced technique, the study not only provides utilities with a robust tool to mitigate potential harm caused by harmonics from renewable energy systems connected to distribution transformers. The proposed model eliminates the reliance on laborious calculations or unreliable sensor data for monitoring hotspot temperatures, offering a significant advancement over conventional approaches. This innovative solution not only enhance the precision of transformer health monitoring but also improve the maintenance strategies and operational dependability. By addressing the limitation of traditional methods, this study represents a critical step forward in ensuring the resilience of transformers in harmonic-rich environments.

2. Model Description

2.1 Test System and Specifications

In the proposed three-phase electrical system, Figure 1 provides a comprehensive view of a three-phase GCPV system, comprising key components such as a three-phase grid source, a 200 kVA 11 kV/400 V three-phase distribution transformer, photovoltaic (PV) panels, an inverter to convert the energy produced by PV panel from DC to AC power source and three-phase unbalanced AC loads. Additional components associated with the PV system are included in the designed block diagram such as a DC-DC boost converter which incorporates the maximum power point tracking (MPPT) to extract the maximum power from solar PV panels, a pulse width modulator (PWM) to generate the controlled pulse of reference current signals to the inverter, and LCL filter to improve the quality of power supplied to the grid. It is worth mentioning that this study models a rectifier supplying passive elements at the consumer side to emulate harmonic loads. The distribution transformer is designed to exhibit the characteristics of a real distribution transformer in a low-voltage network. The parameters, including rated losses and temperature data, are detailed in Table 2. The solar PV system, designed as a grid-connected model, is integrated into the distribution network with appropriately defined parameters.

2.2 Harmonic Loss Model

The formulations related in the power loss calculation are adopted from IEEE Std C57.110-2018 (2018). Power losses of distribution transformer consists of load losses, P_{LL} and no-load losses, P_{NL} basically the total power losses of the distribution transformer, P_T are achieved by the summation of the both losses as in the expression (1).

$$P_T = P_{LL} + P_{NL} \quad (1)$$

Where P_{LL} is the value of load losses where it can be obtained along the operation of the distribution transformer supplying to

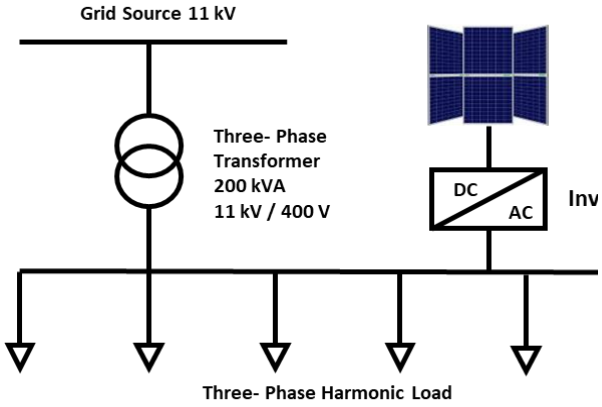

Fig. 1 General Model for Grid-Connected Solar Network

Table 2
Transformer and Solar Panel Specifications

Transformer	
Capacity	200 kVA
Primary Voltage	11,000 V
Secondary Voltage	400 V
Primary Current, I_1	10.5 A
Secondary Current, I_2	288.68 A
Frequency	50 Hz
Short Circuit Capacity, MVA_{sc}	7 MVA
Rated Load Loss, P_{LL-R}	2600 W
Rated No Load Loss, P_{NL-R}	325 W
Rated Ohmic Loss, P_{I^2R-R}	1187.5 W
Rated Eddy Current Loss, P_{EC-R}	847.5 W
Rated Other Stray Loss, P_{OSL-R}	565 W
Ambient Temperature	30 °C
Rated Top Oil Temperature	55 °C
Gradient Temperature	48°C
PV System	
Power Output per Panel	213.5 W
Irradiance	1000 W/m^2
Ambient Temperature, T_A	30°C
Open circuit voltage, V_{oc}	36.3 V
Short-circuit current, I_{sc}	7.84 A
Voltage at maximum power point, V_{MP}	29 V
Current at maximum power point, I_{MP}	7.35 A
No. of MPPT Channel	1
Maximum Efficiency	97%

the load. These losses result in the generation of heat, which increase the temperature of the transformer windings. It consists of ohmic loss, P_{I^2R} eddy current loss, P_{EC} and other stray losses, P_{OSL}.

$$P_{LL} = P_{I^2R} + P_{EC} + P_{OSL} \quad (2)$$

Ohmic loss, often referred as I^2R loss or copper loss, can be defined as the power loss occurs due to the result of the load current flowing through the transformer windings encountering resistance. If the root mean square (RMS) load current increases due to the presence of harmonic components, the ohmic loss will be escalated accordingly.

$$P_{I^2R} = P_{I^2R-R} \sum_{h=1}^{h=max} \left(\frac{I_h}{I_R}\right)^2 \quad (3)$$

Where P_{I^2R-R} is the rated value of ohmic loss, h is the harmonic order, I_h is the RMS value of harmonic current and I_R is the RMS value of current at rated condition. Eddy current loss, P_{EC} is a stray loss in winding components and it is proportional to the square of load current and approximately proportional to the square of harmonic order frequency. Winding eddy current loss is a significant characteristic that causes excessive winding loss and winding temperature rise in transformers supplying non-sinusoidal load currents.

$$P_{EC} = P_{EC-R} \sum_{h=1}^{h=max} \left(\frac{I_h}{I_R}\right)^2 h^2 \quad (4)$$

Where P_{EC-R} is the value of rated eddy current loss. On the other hand, other stray loss, P_{OSL} is commonly recognized in the core, clamps, and other structural parts of the transformer.

$$P_{OSL} = P_{OSL-R} \sum_{h=1}^{h=max} \left(\frac{I_h}{I_R}\right)^2 h^{0.8} \quad (5)$$

Where P_{OSL-R} is the value of rated other stray losses. The heat produced by other stray losses is dissipated through the cooling air, which is why these losses do not affect dry-type transformers. However, these losses may have an impact on liquid-immersed transformers as the losses from the other structural parts of a transformer can further heat the cooling liquid. Meanwhile, P_{NL} is the no-load loss often referred to as core loss, P_C, which is generated due to the magnetization of induced voltage in the core.

$$P_{C-h} = P_{C-R} \times \sum_{h=1}^{h=max} \left(\frac{V_h}{V_R}\right)^m \times \frac{1}{h^{2.6}} \quad (6)$$

Where P_{C-R} are the core losses at rated condition, V_h is the RMS value of voltage at hth harmonic order, and V_R is the RMS value of voltage at rated fundamental frequency, h is the harmonic order and m represents the magnetic characteristic of the distribution transformer's core which lies between the values of 0 and 2 (Dao & Phung, 2018).

2.3 Hotspot Temperature Model from IEEE Standard Formulation

The hottest-spot temperature of a liquid-immersed transformer consists of three main components as represented in Equation (5). According to the standard of IEEE Std C57.91-2011 (2011), the limit of aging factor is established by the reference temperature of 110°C. Moreover, it is important to note that transformers designed for an ONAN cooling system, the empirical constant m and n, are also taken from the standard, which have been empirically specified to the power of 0.8.

$$\theta_{HS} = \theta_A + \theta_{TO} + \theta_G \quad (7)$$

Where θ_{HS} is the winding hottest-spot temperature in °C, θ_A is the average ambient temperature in °C, θ_{TO} is the top-oil rise over ambient temperature in °C and θ_G is the thermal gradient

$$\theta_{TO} = \theta_{TO_R} \times \left[\frac{P_{LL}+P_{NL}}{P_{LL\_R}+P_{NL}}\right]^m \quad (8)$$

Where θ_{TO_R} is the top-oil temperature at rated condition, P_{LL} is the load loss under harmonic condition in kW, P_{NL} is the no-load loss in kW, P_{LL-R} is the rated load loss in kW and m is the winding cooling empirical constant. However, since this study ponders the no-load loss contribution from voltage harmonics, the formulation necessitates the corrected no-load loss value under harmonic conditions in the expression.

$$\theta_{TO} = \theta_{TO_R} \times \left[\frac{P_{LL}+P_{NL}}{P_{LL\_R}+P_{NL\_R}}\right]^{0.8} \quad (9)$$

Where P_{NL} is the no load loss value under harmonic condition in kW and P_{NL-R} is the rated no-load loss value in kW. Meanwhile, the thermal gradient is the winding hottest-spot temperature rise over the top-oil temperature.

$$\theta_G = \theta_{G\_R} \times \left[\frac{P_{LL}}{P_{LL\_R}}\right]^{0.8} \quad (10)$$

Where θ_{G_R} is the rated thermal gradient in °C. it is noteworthy to mention that the insulating liquid temperature rise above ambient temperature shall not exceed 65 °C when measured near the top of the main tank.

2.4 Lifetime Estimation Model

The transformer lifetime expectancy is estimated by utilizing the standardized ageing equation based on the relation of hottest-spot temperature and the winding insulation per-unit life time as expressed in (11), referred from the standard of IEEE Std C57.91-2011 (2011).

$$per\ unit\ life = 9.8 \times 10^{-18} e^{\left(\frac{15{,}000}{\theta H + 273}\right)} \quad (11)$$

Where θH is the hottest-spot temperature in °C. It reflects the aging rate speeds up beyond the standard when the temperature exceeds the reference temperature of 110 °C and the aging rate reduced below the normal when the temperature is below reference temperature. On the other hand, ageing acceleration factor, F_{AA} quantifies the equivalent aging of the transformer

$$F_{AA} = e^{\left(\frac{15000}{383} - \frac{15000}{\theta H + 273}\right)} \quad (12)$$

Where θH is the hottest-spot temperature in °C. F_{AA} indicates value greater than 1 when the HST exceeds temperature reference signifies an increased in aging acceleration of transformer. Conversely, a value less than 1 indicates slower aging acceleration.

2.5 Cost of Transformer Losses

Beyond the technical impact of harmonic-induced losses on transformers thermal stresses and operational lifetime, the economic implications are also considered, particularly in terms of total cost of losses (TCL) (Soleimani & Kezunovic, 2021; Thango *et al*., 2021). Additionally, these losses contribute to increase capital and maintenance cost that must be justified against expected efficiency gains and extended transformer lifespan.

$$TCL = AP_{NL} - BP_{LL} \quad (13)$$

Where A is the assigned cost of no-load losses per watt, P_{NL} is the value of no-load losses, B is the assigned cost of load-losses per watt, and P_{LL} is the value of load losses. The capitalization of no-load and load losses can be expressed as (14) and (15).

$$A = \frac{PW \times C_{kWh} \times 8760}{1000} \quad (14)$$

Where PW is the transformer's present worth and C_{kWh} is the annual cost of energy per kWh.

$$B = \frac{PW \times C_{kWh} \times 8760}{1000} \times \left(\frac{I_L}{I_R}\right)^2 \quad (15)$$

Where I_L is the loading current and I_R is the rated current of the transformer. The present worth (PW) is the deferred monetary expenses influenced by the interest rate and inflation.

$$PW = \frac{1 - \left[\frac{1+a}{1+i}\right]^n}{i - a} \quad (16)$$

Where a is the inflation index, i is the projected interest rate per year and n is the transformer's lifetime in years.

Table 3
Transformer and Solar Panel Specifications

Case	PV panel String-Series Configurations	Peak Inverter Output (kW)	Penetration per Full Load Rating (%)
1	-	0	0
2	3-16	10.23	33.33
3	6-16	20.46	66.66

2.5 Case Study

This study evaluates the harmonic content levels in transformers under varying conditions of photovoltaic (PV) integration using Fast Fourier Transform (FFT) analysis. The analysis considers three distinct scenarios, each representing a different level of PV penetration and inverter output power. Case 1 models a transformer operating in a conventional grid without PV integration, serving as a baseline. Cases 2 and 3 simulate grid-connected PV (GCPV) systems with varied PV penetration levels achieved through configuring PV panels to generate different peak inverter output as percentages of the transformer's full load rating (Majeed *et al*. 2022). These configurations and the corresponding penetration levels, calculated as a percentage of total load, are outlined in Table 3. This simulation-based approach ensures a controlled assessment of harmonic impacts under predefined conditions.

3. Proposed Electro-Thermal Model

3.1 Finite Element Analysis (FEA) Implementation

The electro-thermal approach of distribution transformers is conducted using Finite Element Analysis using COMSOL Multiphysics software to examine the impact of harmonic distortion on insulation transformer temperature rise. A two-dimensional cross-sectional model of an oil-immersed, three-phase distribution transformer is created to simulate a real distribution transformer. By initializing appropriate material properties, initial conditions, and boundary settings, the enormous complexity in the geometry design is reduced while maintaining the accuracy of the results (Comsol, 2022). The implementation of FEA for HST simulation for the distribution transformer begins with parameter initialization, where the necessary simulation parameters are defined. Subsequently, the two-dimensional cross-sectional geometry of the transformer is designed, incorporating vital components such as cores, windings, and coolant. Next, the relevant material properties are then assigned, including the iron core, copper winding domain, and transformer oil as a coolant. Following this, a Multiphysics setting is established, integrating various physical phenomena involved in the simulation such as heat transfer, electromagnetic heating, and magnetic field physics settings. The boundary and initial conditions are defined based on corresponding values of transformer losses and temperature conditions, setting the stage for accurate simulation conditions. A computational grid is then generated through mesh creation, after which the simulation is executed and monitored for convergence. Once convergence is achieved, the results are analyzed to interpret the outcomes. Finally, the process concludes, marking the end of the simulation procedure. Figure 2 illustrates the workflow of the FEA implementation.

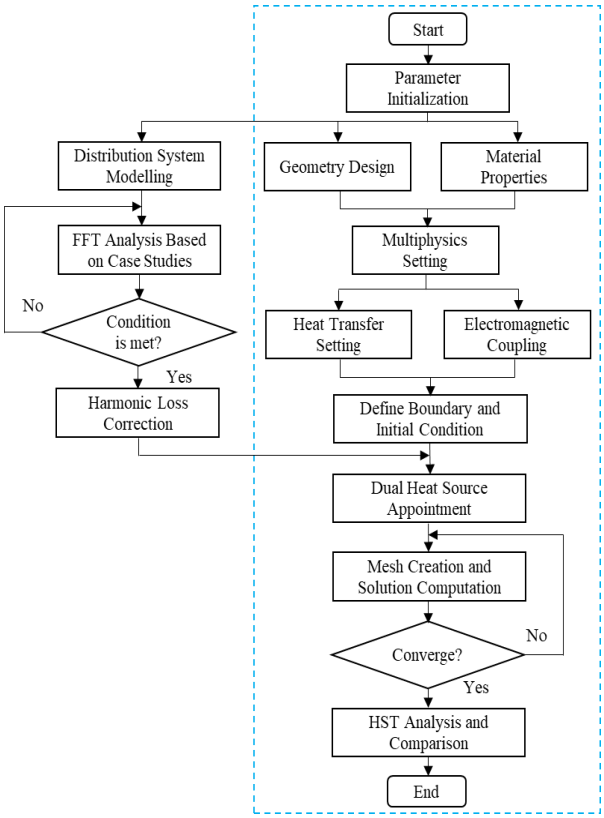

Fig. 2 FEA Implementation in the Proposed Study

3.2 Geometry Design and Material Properties Setting

The transformer thermal model is created using a finite element method (FEM) approach and represents a two-dimensional cross-section of a three-phase liquid-immersed transformer. The model includes three limbs of the transformer core, each corresponding to a phase, with concentric circles within each limb representing the windings. The surrounding area is filled with transformer coolant. Figure 3 illustrates a finely meshed geometric model, designed for a comprehensive heat transfer study. Each of the three circular regions corresponds to an individual transformer phase, encapsulated within a robust grid that enables precise thermal and fluid dynamic analyses, with the courtesy of material properties setting as demonstrated in Table 4. The properties of each material are chosen to match the criteria of the thermal model and suit the problem to be solved in this research. For instance, the relative permeability indicates the tendency of the material to pass in free space, which explains the higher value required for the iron domain to support the formation of the magnetic field. Meanwhile, the relative permittivity defines the quantity of the energy that can be deposited in the material of particular equipment, where the nature value is 1. Electrical conductivity defines a material's ability to conduct electric current, explaining zero conductivity for the transformer oil coolant domain. On the other hand, the heat capacity at constant pressure, represents the heat supplied by the model while maintaining a constant pressure, implying the heat transfer within and outside the model occurs gradually. It is also worth mentioning that some material properties of the oil domain such as heat capacity, density, and thermal conductivity are similar to those of copper and iron. This is due to the oil domain practically overriding the other two domains in the model.

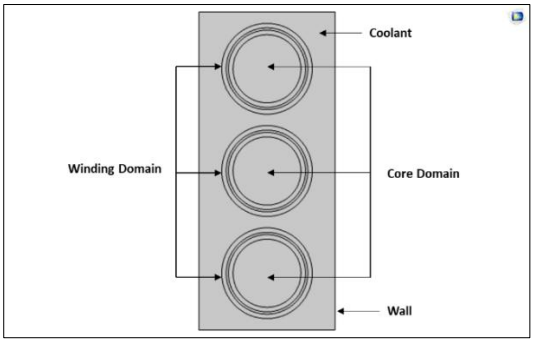

Fig. 3 Geometry Design Electro-Thermal Model

3.3 Multiphysics Implementation

The transformer model is simulated with the employment of coupled heat transfer and electromagnetic equations. The mathematical expressions for the heat transfer study are expressed in (17) and (18), respectively (Said *et al.* 2020).

$$d_z \rho C_p \frac{\partial T}{\partial t} + d_z \rho C_p u.\nabla T + \nabla.q = d_z Q + q_0 + d_z Q_{ted} \quad (17)$$

$$\rho C_p \frac{\partial T}{\partial t} + \rho C_p u.\nabla T = \nabla.(k\nabla T) + Q_e \quad (18)$$

Where d_z is the thickness of the geometry which has been uniformly set to 1metre, ρ is the density, C_p is the specific heat capacity at constant pressure, u is the thermal heat coefficient, T is the temperature, q is the conductive heat flux, Q is the heat source, q_0 is the convection heat flux, k is the thermal conductivity, Q_{ted} is the thermo-elasticity damping which normally being neglected in general practical problem, and the last but not least, Q_e is the electromagnetic heat source.

3.4 Boundary Condition Settings

The computational problem of the electro-thermal model can be accurately solved by selecting appropriate boundary conditions. For this thermal model, both Neumann and Dirichlet boundary conditions are applied for the core and the winding, as shown by the blue lines (Das & Chatterjee, 2017) in Figure 4. The heat

Table 4
Material Properties of Electro-Thermal Model

Property	Domain Material		
	Copper	Iron	Oil
Relative permeability	1	4000	1
Relative permittivity	1	1	1
Electrical conductivity ($\frac{S}{m}$)	5.998×10^7	1.120×10^7	0
Heat capacity at constant pressure ($\frac{J}{kg.K}$)	385	440	Overrides Copper and Iron
Density ($\frac{kg}{m^3}$)	8940	7870	Overrides Copper and Iron
Thermal conductivity ($\frac{W}{m.K}$)	400	762	Overrides Copper and Iron

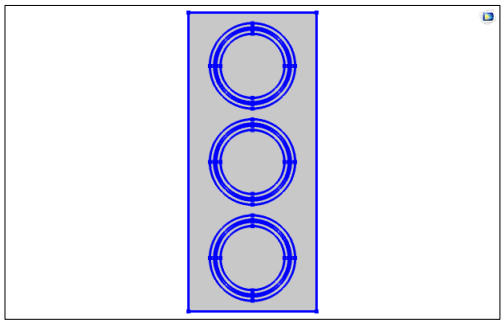

Fig. 4 Boundary Condition Settings

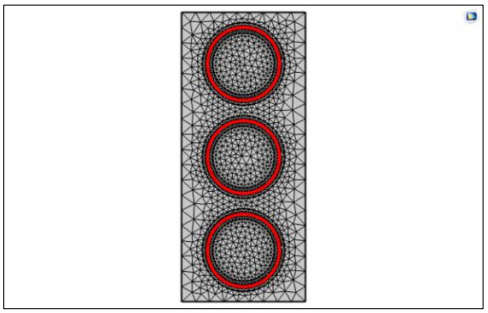

Fig. 6 Mesh Creation and HST Evaluation Region

boundary conditions reflect the thermal insulation of the domains, preventing any energy interchange with the surrounding environment. In this scenario, the heat flux, q across the boundaries vector, n has been disabled and becomes zero.

$$-n.q = 0 \quad (19)$$

3.5 Dual Heat Source Appointment Based on Harmonic Losses

A novel dual heat source approach is employed for this study to accurately simulate the hottest spot temperature in the transformer due to the combined impact of current and voltage harmonics. This approach represents the simultaneous impact of both current and voltage harmonics on the HST, allowing for a more comprehensive assessment of the thermal stress induced by harmonic distortions, thereby enhancing the state-of-the-art techniques of temperature rise monitoring, which considers only one in isolation (Abdali *et al*., 2024; Said *et al*., 2020). The first heat source, as shown in Figure 5(a), is attributed to load loss resulting from the composition of current harmonics, which occur owing to non-linear loads and

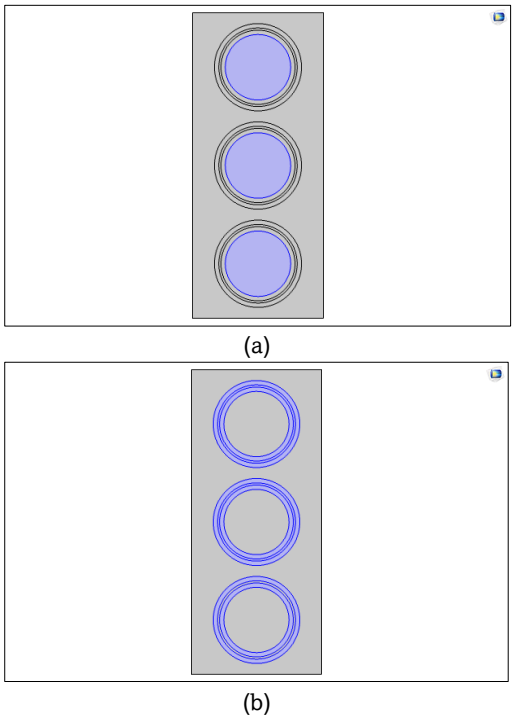

Fig 5 Dual Heat Source Appointment (a) Core Domain (b) Winding Domain

significantly impact the thermal profile of the transformer windings. The second heat source, which is demonstrated in Figure 5(b) originates from no-load loss due to voltage harmonics, which arise as an additional aspect from distortions in the supply voltage waveform and induce additional core losses even in the absence of loads. Therefore, the heat sources, which represented as Q_0 are being applied specifically on the winding and core simultaneously as depicted. The heat sources are defined as the heat rate of harmonic losses, P_0 over volume, V as expressed in Equation (20).

$$Q_0 = \frac{P_0}{V} \quad (20)$$

3.6 Mesh Creation and HST Evaluation for Solution Computation

Finally, the thermal model was segmented into physics-controlled meshes, using a fine element size. This mesh creation is crucial for capturing the complex interactions between the solid and liquid phases, facilitating a greater understanding of thermal distribution and cooling efficiency. Regarding the HST evaluation, the selected region on the thermal model, as shown in red colour in Figure 6, represents the transformer's winding insulation, where an abnormal temperature rise is anticipated (Skillen *et al.* 2012). This temperature transition is driven by the dynamic heat source injections from copper and winding components. Therefore, by referring to the limit standard, the compliance of the HST is demonstrated throughout the simulation based on the heat transfer study.

4. Results and Discussion

This section presents a detailed analysis of harmonics in both voltage and current, followed by the assessment of transformer losses attributable to these harmonics. Finally, the electro-thermal model is employed to determine the hottest-spot temperature of the transformer's winding insulation, offering insights into their implications for thermal efficiency and operational integrity.

4.1 Transformer Harmonic and Loss Analysis

Figure 7(a) illustrates the harmonic current magnitude distribution across three distinct cases, each corresponding to a different condition. In Case 1, characterized by the absence of PV penetration and solely influenced by harmonic load, the transformer experiences minimal harmonic currents across all harmonic orders, with the highest value recorded at the 3rd harmonic at 2.78%. this minimal distortion is reflected in the overall total current harmonic distortion (THDi) of 2.99%. In Case 2, with the introduction of PV into the system, a moderated level of harmonic emerges, characterized by noticeable peaks at

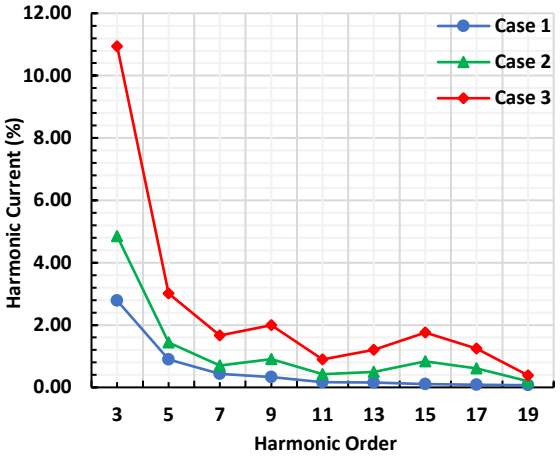

(a)

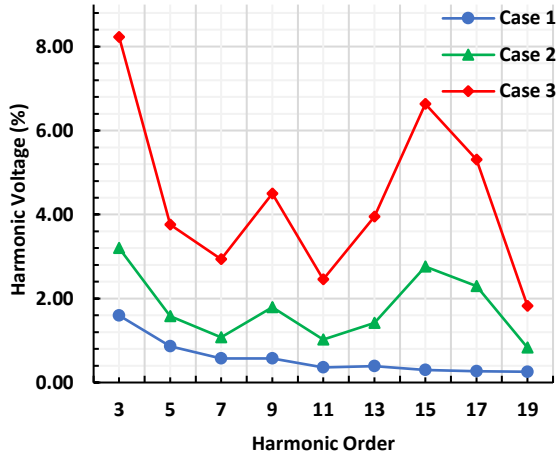

(b)

Fig. 7 Individual Odd Harmonic Evaluation (a) Current (b) Voltage

the 3rd and 5th harmonic orders, reaching 4.85% and 1.44%, leading to a higher THDi of 7.58%. the increase is attributed to the interaction between the PV inverter switching characteristics and the grid, which introduces additional harmonic components. The impact of high PV penetration is most evident in Case 3, where harmonic distortion is significantly elevated. The 3rd harmonic current magnitude exceeds 10%, and there are consistently higher harmonic currents across all orders, resulting in a THDi of 12.05%. This trend proves that as the PV penetration increases, the inverter-driven harmonics become more dominant, intensifying overall system distortion. Following the analysis of harmonic currents, Figure 7(b) illustrates the distribution of harmonic voltage magnitudes for the cases. In Case 1, the voltage harmonics is minimal, with the 3rd harmonic at 1.60%, corresponding to an overall total voltage harmonic distortion (THDv) of 2.44%. The trend shifts in Case 2 where voltage harmonics become pronounced, particularly at the 5th, 9th, and 15th orders, each ranging between 1% and 2%, resulting in a THDv of 6.65%. Case 3 presents the most significant distortion, with notable peaks at the 3rd and 15th harmonics, reaching 8.23% and 6.63%, respectively, leading to a pointedly higher THDv of 16.43%. This case also displays a broader distribution of elevated harmonic magnitudes across the lower to higher orders, underscoring the more severe impact of distortion.

Table 5
Transformer Harmonic Loss Evaluation

Case	Type of Loss	Rated Value (W)	Real Value (W)	Corrected Value (W)
1	P_{LL}	2600	2612.39	2622.88
	P_{NL}	325	325.33	325.33
	Total	2925	2937.72	2948
2	P_{LL}	2600	2666.89	2730.19
	P_{NL}	325	326.14	326.14
	Total	2925	2993.03	3056.33
3	P_{LL}	2600	2921.15	3289.53
	P_{NL}	325	329.57	329.57
	Total	2925	3250.72	3619.09

The impact of harmonics on the distribution transformer is assessed through harmonic loss evaluation, as detailed in Table 5. The rated value represents the baseline loss value, excluding unusual factors to provide a reference for comparison. Notably, the harmonic loss factor is applied exclusively to winding eddy current losses and other stray losses, as ohmic losses are frequency-independent and directly proportional to the current, typically addressed by considering the increased RMS current due to harmonic components. This assumption aligns with transformer loss models and ensures that the analysis accurately reflects the primary sources of additional losses under harmonic conditions. Based on the rated values, the total enhanced loss, encompassing both load and no-load losses, is calculated. The results indicate a clear trend, as the harmonic levels rise, the additional losses incurred by the transformer increase. For instance, in Case 1, representing a conventional grid distribution transformer without PV input, the additional loss is minimal, approximately 0.36%. In contrast, Case 2, involving a PV system with 33.33% peak inverter output, shows a significant escalation in additional loss of 2.11%. This increase is attributed to the harmonic current generated by the PV inverter, which elevate winding eddy current and stray losses, reinforce the assumption that inverter-induced harmonics significantly impact transformer efficiency. The highest additional loss is observed in Case 3, with a peak inverter output is increased to 66.67%, demonstrating a strong correlation between higher PV capacities and increased transformer loss, where the additional accumulated losses incurred in the transformer reach 12.61%. These findings are consistent with previous studies, such as those by Sanjay Kulshreshtha & Dr D.K Chaturvedi (2024) and (Loaena, 2017), who also reported a proportional relationship between harmonic distortion levels and transformer losses. The escalation in values reinforces the progression of additional losses as harmonic distortion intensifies, further supporting the correlation between higher harmonic levels and the degradation in transformer performance, which will be discussed in the next section.

4.2 Hotspot Temperature Analysis Using Proposed Method

The hottest-spot temperature behavior is observed based on the harmonic composition from each case. It is important to recall that the reference temperature of 110°C indicates the threshold at which the aging rate of transformer insulation accelerates beyond the standard, whereas operation below this threshold reduces the aging rate (Institute of Electrical and Electronics Engineers, 2022). Conclusively, the graph depicted in Figure 8 summarizes the hottest-spot temperature (HST) behavior in a transformer subjected to three different harmonic conditions, influenced by PV system integration. The time to reach this critical temperature varies significantly across the three cases,

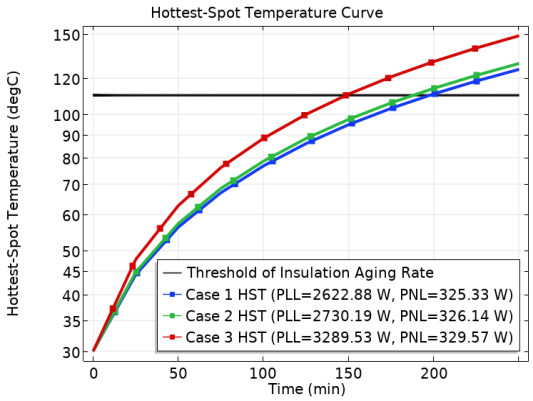

Fig. 8 Time-Dependent HST Analysis for each case.

indicating the profound impact of harmonic distortions on transformer heating.

Figure 9(a) demonstrates the contour simulation of the hottest spot in a transformer up to 250 minutes under the influence of harmonic conditions from Case 1, where the heat source from load loss and no-load loss are 2622 W and 325 W, respectively. Initially, the temperature rises gradually from the ambient temperature of 30°C, showing a steady increase that becomes more pronounced as time progresses. The winding insulation temperature reaches the IEEE aging factor temperature at approximately the 200th minute. This slower temperature rise is indicative of minimal harmonic losses. Under low harmonic conditions, the additional losses generated by harmonic currents are relatively small, allowing the transformer to operate closer to its nominal thermal performance. By the end of the simulation, the hottest spot temperature approaches 125.46°C. Consequently, the temperature increment is gradual, taking longer to reach the critical 110°C mark. This upward trend highlights the impact of harmonic loads on transformer heating. However, it is noteworthy that the temperature remains below the normal insulation reference temperature of 110°C throughout the observed period until the 200th minute. However, the rapid temperature increase towards the end of the period warrants attention to ensure continued safe operation under prolonged exposure to such loads.

On the other hand, Figure 9(b) illustrates the contour simulation of the hottest spot in a transformer under harmonic conditions from Case 2, with the increased load and no-load loss of 2730 W and 326 W, respectively. The curve's upward trajectory signifies the continuous heating of the transformer, with the hottest spot temperature nearing the critical insulation reference temperature of 110°C towards the end of the simulation period at the value of 129.24°C, while the winding insulation temperature surpasses the reference temperature around the 178th minute. This intermediate behavior suggests a moderate level of harmonic distortions, which contributes higher additional losses compared to Case 1. The increased losses from harmonics accelerate the heating process, causing the HST to rise more quickly. This earlier crossing point highlights the escalating impact of harmonics, where moderate levels already cause noticeable deviations from the ideal thermal performance This trend emphasizes the significant thermal impact of harmonic loads on the transformer. Importantly, while the temperature approaches the normal insulation reference limit of 110°C, it does not exceed it, indicating that the transformer remains within its safe operational limits during the simulated time frame. However, the close proximity to the insulation limit towards the end suggests the necessity for careful monitoring and potentially enhanced cooling strategies to ensure sustained safe operation under prolonged harmonic loading.

Meanwhile, Figure 9(c) depicts the contour simulation of the hottest spot in a transformer subjected to Case 3 condition, where the load loss and the no-load loss values are escalated to 2730 W and 326 W, respectively. The data points, reveal a consistent rise in temperature starting from 30°C, reaching the value of 148.80°C by the end of the simulation period. This temperature surpasses the normal insulation reference temperature roughly at the 149th minute, showcasing the steepest temperature rise among the three cases. This rapid increase in HST is due to the highest level of harmonic distortions, which introduce substantial additional losses. High harmonic conditions lead to significant heating effects as the transformer experiences increased core losses and copper losses. The resultant thermal stress not only accelerates the temperature rise but also poses a risk of overheating, potentially shortening the transformer's lifespan and compromising its reliability. The differences in temperature rise rates and the

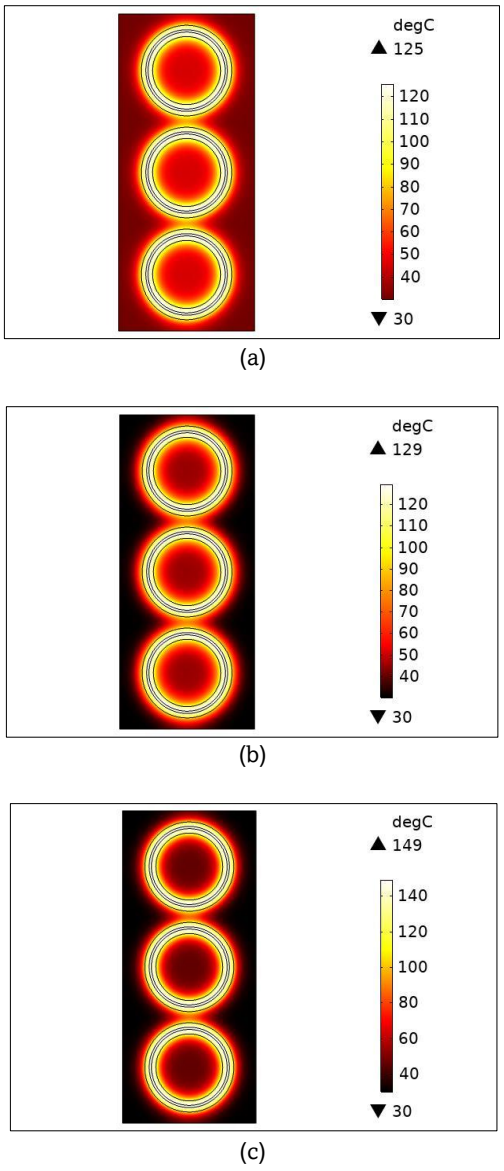

Fig. 9 Contour Simulation (a) Case 1 (b) Case 2 (c) Case 3

Table 6
Comparison of Proposed Method against Mathematical Approach

Case Study	Final Hottest-Spot Temperature via Proposed Model (°C)	Final Hottest-Spot Temperature via Mathematical Model (°C)	Similarity Percentage (%)
1	125.46	124.84	99.51
2	129.24	127.78	98.87
3	148.8	142.66	95.87

respective times of crossing the reference temperature across the three cases underscore the critical influence of harmonic distortions on transformer thermal performance. Higher harmonic conditions cause greater additional losses, leading to faster temperature increases and earlier crossing points of the critical 110°C threshold. These findings align with previous studies, including those conducted by Awadallah *et al.* (2016), which reported increase in hottest-spot temperatures due to harmonic distortion from solar panel operation compared to normal condition. The variations underscore the sensitivity of the transformer's thermal performance to the specific harmonic content introduced by PV integration, highlighting the need for careful consideration of these factors in modern power systems**.**

4.3 Comparison of Hottest-Spot Temperature with Mathematical Approach

Before the evaluation of the operational lifetime, it is necessary to validate the HST evaluation using FEA method results for hotspot temperature in COMSOL against the mathematical analysis through the IEEE C57.110-2018 standard, as demonstrated in Table 6. The comparison of hottest-spot temperature refers to the final insulation temperature based on the time-dependent study against the mathematical calculations through the IEEE standard formulations, which utilize the aforementioned rated loss values and expressions. This comparison demonstrates the high degree of accuracy of the FEA method, with similarity percentages exceeding 95% across all case studies. This strong correlation validates the reliability of the FEA approach, confirming that it can produce highly accurate results for transformer HST, effectively reducing the need for labor-intensive manual calculations and expensive laboratory tests. Furthermore, the close agreement between the two methods underscores the capability of the proposed method to provide a dependable indication of the transformer's thermal condition, ensuring efficiency in predicting transformer lifespan and preventing premature failures.

4.4 Transformer Lifetime Estimation Analysis

The lifetime estimation of the distribution transformer is observed by referring to the relationship between the hottest-spot temperature (HST), winding insulation per-unit lifetime, and aging acceleration factor. Since insulation degradation is directly linked to temperature rise, evaluating these parameters provides crucial insights into the long-term reliability of the transformers under different harmonic conditions. Figure 10 (a) and Figure 10(b) compare the per-unit (PU) life and aging acceleration factor (FAA) of the transformer for each case respectively. These metrics are evaluated based on the final HST from proposed method and IEEE standard formulations. The analysis reveals progressive degradation in transformer performance and accelerated aging due to aforementioned scenarios. For instance, in the conventional grid of Case 1, the corresponding per-unit life for the transformer is 0.2189 and 0.2321 for the proposed and IEEE methods, respectively. This indicates a relatively low reduction in lifetime. The FAA is also low, at 4.5702 and 4.3098, respectively. Meanwhile, with the integration of the PV system, there is a noticeable increase in the thermal stress in Case 2. The per-unit life values of the corresponding transformer decrease to 0.1357 and 0.1760, respectively. This shows a significant reduction in the transformer lifespan owing to the increased harmonic content. This is further corroborated by the rise in FAA, which increases to 6.510 for the proposed method and 5.682 for the IEEE model. Finally, in the increased PV inverter output scenario, the transformer undergoes severe stress, as reflected by the highest reach of HST. The PU life dropped intensely to 0.0273 for the proposed method and 0.0461 for the IEEE model, indicating substantial aging and reduced operational reliability. Meanwhile, the value of FAA experienced a sharp increase to 36.69 and 21.70, respectively. These significant increases indicate an exponential acceleration of insulation degradation, emphasizing that higher distortions drastically shorten transformer service life. These findings are comparable to an existing study by Taheri *et al.* (2019), which reported a range of

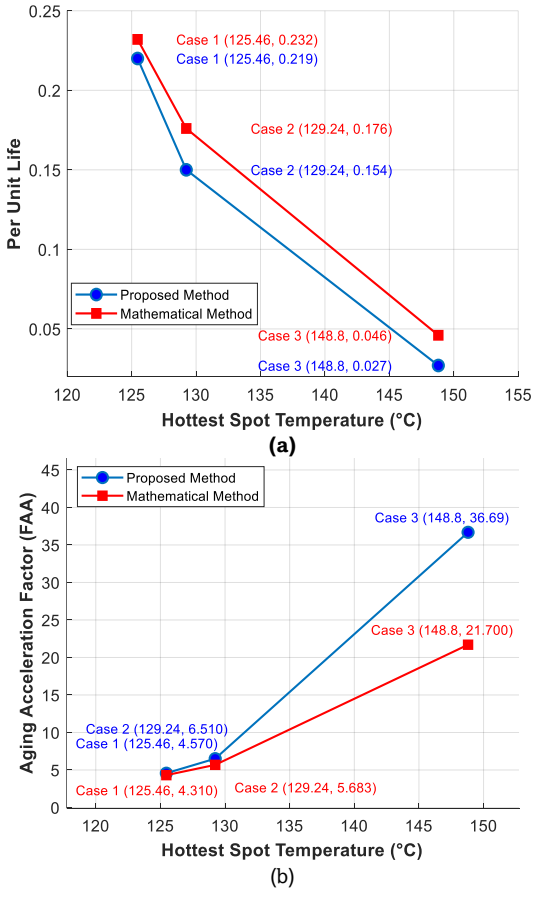

Fig. 10 (a) Per Unit Life Curve **(b)** Aging Acceleration Factor Curve

34.46%-42.64% increase in the loss of life reduction due to solar radiation. This drastic change underscores the severe effect of excessive harmonic distortions from the PV inverter output, particularly at higher levels of generation. The results illustrate the profound impact of PV integration and increased inverter output on transformer aging and performance. As PV systems are integrated into the grid, the harmonic distortions contribute to elevated HST values, leading to reduced PU life and increased FAA.

4.5 Economic Evaluation on Cost of Transformer Losses

The economic impacts of harmonic-induced losses extend beyond increased energy costs, as they directly influence the transformer's expected lifetime and premature failure. The total cost of losses (TCL) can be assessed under both rated and harmonic-induced conditions by relating the harmonic loss composition. Therefore, the cost of losses is determined from the harmonic losses in both rated and harmonic-induced conditions, the investment index, the interest rate, and the annual energy cost. This approach ensures a comprehensive evaluation of the financial implications of harmonics, considering both direct energy-related expenses and long-term asset depreciation. Table 7 presents the characteristic parameters used for cost evaluation. Table 8 depicts the comparison of the total cost of transformers due to different harmonic conditions. The assigned cost of no-load loss, A, and the assigned cost of load loss, B, are determined as 38.193 and 7.941, respectively. These values are primarily derived based on the cost of energy per year, investment index, and interest rate. Since A and B serve as fixed multipliers for evaluating the loss-related costs, they remain unchanged irrespective of harmonic conditions in each case. Under rated operating conditions, the total loss is 2937 W, resulting in a total cost of losses is RM33,153.74, which serves as a baseline for comparison. The cost of losses increases as harmonic distortion increases across case studies. In Case 1, where the cumulative harmonic loss is 2948.21 W, the cost increases from RM 33153.74 to RM 33252.74. However, in Case 2, the increased cumulative harmonic losses of 3056.33 W result in a higher cost of losses, reaching RM 34135.79. The trend intensified in Case 3, where the cumulative harmonic losses further increased to 3619.10 W, driving the cost to RM 38708.33, highlighting the substantial economic impact of harmonics. These cost variations align with the reduction in per-unit lifetime, which decreases from 0.2189 in Case 1 to 0.1537 in Case 2 and drops to 0.0273 in Case 3. This sharp decline in transformer lifespan under high harmonic conditions demonstrates the long-term financial risks associated with excessive harmonic distortions, consistent with the findings of Soleimani & Kezunovic (2021) and Thango *et al.* (2021). Based on these observations, it can be deduced that the presence of harmonic adversely influences both the technical and economic efficiencies of transformers. These explorations emphasize the importance of exploring solutions that not only enhance technical performance but also mitigate the economic burden imposed by the utility.

5. Conclusion

This paper presents an advancement in the electro-thermal design of distribution transformers by introducing an improved method for evaluating HST under the influence of harmonic distortions, specifically from PV system integration. The dual heat source approach, which accounts for both the core and winding domains, enhances the precision of HST estimation, offering a more detailed understanding of the thermal stresses imposed on transformer winding insulation. Through a comprehensive time-dependent analysis using COMSOL Multiphysics, it was demonstrated that the harmonics led to a notable elevation in the HST, with distinct variations in trends across different harmonic levels. In Case 3, characterized by the highest harmonic level, the HST reaches the normal insulation reference temperature significantly faster than Case 2 and Case 1, where harmonic levels are moderate and low, respectively. This rapid rise in HST in Case 3 correlates with a dramatic reduction in per-unit life, from 0.219 in Case 1 to 0.027, and an

Table 7
Economic Evaluations Parameters

Description	Value
Cost of Energy, C_{kWh} (RM/year)	0.437/kWh
Rating Current, I_R (A)	288.68
Loading Current, I_l (A)	131.63
Inflation Index, a (%)	3.1
Interest Rate, i (%)	10

Table 8
Cost Comparison Based on Different Cases

Parameter	Conditions			
	Rated	Case 1	Case 2	Case 3
No-Load Loss Capitalization, A (RM/W)	38.193	38.193	38.193	38.193
No-Load Loss (W)	325.00	325.33	326.14	329.57
Load Loss Capitalization, B (RM/W)	7.941	7.941	7.941	7.941
Load Loss (W)	2612	2622.88	2730.19	3289.53
Cost of Losses (RM)	33153.74	33252.74	34135.79	38708.33

increase in the acceleration factor from 4.310 to 21.7. This increase in temperature has a direct correlation with the potential for premature transformer failure, as validated by comparison with IEEE-based formulations. With a similarity of more than 95%, the model reliably mirrors IEEE formulations, confirming its robustness and consistency in thermal-stress prediction.

However, it is important to acknowledge the limitations of this study. This analysis proposes a model assuming constant ambient conditions and idealized oil-type transformer behavior, which may not fully capture the complexities of real-world operating environments. Variations in ambient temperature, load fluctuations, and non-ideal transformer characteristics could influence the results. These assumptions simplify the analysis but may restrict the applicability of the findings to more diverse and complex grid conditions. Moreover, future work may include a detailed financial analysis of transformer efficiency losses and the cost of potential mitigation strategies such as harmonic filtering or optimized loading practices. Despite these limitations, this advancement provides utility engineers and researchers with a reliable predictive tool to assess and mitigate thermal stress-related transformer failures in PV-integrated power systems. Furthermore, the insights gained from this study can guide the development of design and operational strategies to enhance transformer resilience, such as optimized loading practices or harmonic filtering solutions, in environments with significant harmonic distortion. Future studies could build upon this work by refining the model and exploring advanced mitigation techniques to address challenges in harmonic-rich networks, further supporting the deployment of renewable energy systems.

Acknowledgments

This paper was developed in the laboratory of Central Electrical Energy Systems (CEES), Faculty of Electrical Engineering, Universiti Teknologi Malaysia.

Author Contributions: All authors contributed equally in developing this paper. The final version of the manuscript was read and approved by all authors.

Funding: This work was conducted under the funded research grant Q.J130000.3009.04M67.

Conflicts of Interest: The authors declare no conflict of interest.

References

Abdali, A., Mazlumi, K., & Rabiee, A. (2024). Harmonics impact on hotspot temperature increment of distribution transformers: Nonuniform magnetic-thermal approach. *International Journal of Electrical Power and Energy Systems*, *157*. https://doi.org/10.1016/j.ijepes.2024.109826

Ackermann, T., Ran Andersson, G., & Sö Der A, L. (2001). Distributed generation: a definition. *Electric Power Systems Research*, 57. www.elsevier.com/locate/epsr

AJ, C., Salam, M. A., Rahman, Q. M., Wen, F., Ang, S. P., & Voon, W. (2018). Causes of transformer failures and diagnostic methods – A review. In *Renewable and Sustainable Energy Reviews*, 82, 1442–1456. https://doi.org/10.1016/j.rser.2017.05.165

Américo, J. P., Leite, J. V., & Mazzola, C. F. (2024). Enhanced thermal modeling of three-phase dry-type transformers. *Case Studies in Thermal Engineering*, *58*. https://doi.org/10.1016/j.csite.2024.104445

Awadallah, M. A., Venkatesh, B., & Singh, B. N. (2015). Impact of solar panels on power quality of distribution networks and transformers. *Canadian Journal of Electrical and Computer Engineering*, *38*(1), 45–51. https://doi.org/10.1109/CJECE.2014.2359111

Awadallah, M. A., Xu, T., Venkatesh, B., & Singh, B. N. (2016). On the Effects of Solar Panels on Distribution Transformers. *IEEE Transactions on Power Delivery*, *31*(3), 1176–1185. https://doi.org/10.1109/TPWRD.2015.2443715

Cazacu, E., Ionita, V., & Petrescu, L. (2018). *Thermal Aging of Power Distribution Transformers Operating under Nonlinear and Balanced Load Conditions*. https://doi.org/10.15598/aeee.v16i1.2701

Chen, T., Liu, Z., Wang, P., Jiang, J., & Yang, F. (2023). Temperature Simulation of 800 kVA Converter Transformer Windings Considering the Effects of High-Order Harmonics. *2023 26th International Conference on Electrical Machines and Systems, ICEMS 2023*, 2589–2593. https://doi.org/10.1109/ICEMS59686.2023.10344825

Comsol. (2022). *The Heat Transfer Module User's Guide*. https://doc.comsol.com/6.1/doc/com.comsol.help.heat/HeatTransferModuleUsersGuide.pdf

Dao, T., & Phung, B. T. (2018). Effects of voltage harmonic on losses and temperature rise in distribution transformers. *IET Generation, Transmission and Distribution*, *12*(2), 347–354. https://doi.org/10.1049/iet-gtd.2017.0498

Das, A. K., & Chatterjee, S. (2017). Finite element method-based modelling of flow rate and temperature distribution in an oil-filled disc-type winding transformer using COMSOL multiphysics. *IET Electric Power Applications*, *11*(4), 664–673. https://doi.org/10.1049/iet-epa.2016.0446

El Batawy, S. A., & Morsi, W. G. (2017). On the impact of high penetration of rooftop solar photovoltaics on the aging of distribution transformers. *Canadian Journal of Electrical and Computer Engineering*, *40*(2), 93–100. https://doi.org/10.1109/CJECE.2017.2694698

Fortes, R. R. A., Buzo, R. F., & de Oliveira, L. C. O. (2020). Harmonic distortion assessment in power distribution networks considering DC component injection from PV inverters. *Electric Power Systems Research*, *188*. https://doi.org/10.1016/j.epsr.2020.106521

Gorginpour, H., Ghimatgar, H., & Toulabi, M. S. (2022). Lifetime Estimation and Optimal Maintenance Scheduling of Urban Oil-Immersed Distribution-Transformers Considering Weather-Dependent Intelligent Load Model and Unbalanced Loading. *IEEE Transactions on Power Delivery*, *37*(5), 4154–4165. https://doi.org/10.1109/TPWRD.2022.3146154

Hajipour, E., Mohiti, M., Farzin, N., & Vakilian, M. (2017). Optimal distribution transformer sizing in a harmonic involved load environment via dynamic programming technique. *Energy*, *120*, 92–105. https://doi.org/10.1016/j.energy.2016.12.113

Hamza, E. A., Sedhom, B. E., & Badran, E. A. (2021). Impact and assessment of the overvoltage mitigation methods in low-voltage distribution networks with excessive penetration of PV systems: A review. *International Transactions on Electrical Energy Systems* 31(2). https://doi.org/10.1002/2050-7038.13161

Hossain, M. S., Abboodi Madlool, N., Al-Fatlawi, A. W., & El Haj Assad, M. (2023). High Penetration of Solar Photovoltaic Structure on the Grid System Disruption: An Overview of Technology Advancement. *Sustainability (Switzerland)* 15(2). https://doi.org/10.3390/su15021174

IEEE Std C57.91-2011*(Revision of IEEE Std C57.91-1995) : IEEE Guide for Loading Mineral-Oil-Immersed Transformers and Step-Voltage Regulators Sponsored by the Transformers Committee*. (2011). IEEE.

IEEE Std C57.110-2018 *(Revision of IEEE Std C57.110-2008) : IEEE Recommended Practice for Establishing Liquid-Immersed and Dry-Type Power and Distribution Transformer Capability When Supplying Nonsinusoidal Load Currents*. (2018). IEEE.

IEEE Std C57.12.00-2021 - IEEE *Standard for General Requirements for Liquid-Immersed Distribution, Power, and Regulating Transformers*. (2022). IEEE.

León-Martínez, V., Peñalvo-López, E., Montañana-Romeu, J., Andrada-Monrós, C., & Molina-Cañamero, L. (2023). Assessment of Load Losses Caused by Harmonic Currents in Distribution Transformers Using the Transformer Loss Calculator Software.

Environments - MDPI, *10*(10). https://doi.org/10.3390/environments10100177

Liu, C., Hao, J., Liao, R., Yang, F., Li, W., & Li, Z. (2024). High proportion and large value harmonic current influence on the magnetic field, loss and temperature distribution for ultrahigh voltage converter transformer. *IET Electric Power Applications*, *18*(2), 208–225. https://doi.org/10.1049/elp2.12382

Loaena, Y. G. (2017). Evaluation of Harmonics & Its Effect on Transformer Load Loss. *Journal of Energy Technologies and Policy*, *7*(8). www.iiste.org

Lu, P., Buric, M. P., Byerly, K., Moon, S. R., Nazmunnahar, M., Simizu, S., Leary, A. M., Beddingfield, R. B., Sun, C., Zandhuis, P., McHenry, M. E., & Ohodnicki, P. R. (2019). Real-Time Monitoring of Temperature Rises of Energized Transformer Cores with Distributed Optical Fiber Sensors. *IEEE Transactions on Power Delivery*, *34*(4), 1588–1598. https://doi.org/10.1109/TPWRD.2019.2912866

Majeed, I., & Nwulu, N. (2022). Impact of Reverse Power Flow on Distributed Transformers in a Solar Photovoltaic Integrated Low Voltage Network. *SSRN Electronic Journal*. https://doi.org/10.2139/ssrn.4172636

Panigrahi, R., Mishra, S. K., Srivastava, S. C., Srivastava, A. K., & Schulz, N. N. (2020). Grid Integration of Small-Scale Photovoltaic Systems in Secondary Distribution Network - A Review. *IEEE Transactions on Industry Applications*, *56*(3), 3178–3195. https://doi.org/10.1109/TIA.2020.2979789

Ruiz, I. R. M., Guajardo, L. A. T., Alfaro, L. H. R., Salinas, F. S., Maldonado, J. R., & Vázquez, M. A. G. (2021). Design implication of a distribution transformer in solar power plants based on its harmonic profile. *Energies*, *14*(5). https://doi.org/10.3390/en14051362

Said, D. B. M., Yassin, Z. I. M., Ahmad, N., Abd Malik, N. N. B. N., & Abdullah, H. (2020). Impact of unbalanced harmonic loads towards winding temperature rise using fem modeling. *Indonesian Journal of Electrical Engineering and Informatics*, *8*(2), 409–418. https://doi.org/10.11591/ijeei.v8i2.1283

Sanjay Kulshreshtha, & Dr D.K Chaturvedi. (2024). Effect of Generated Harmonics On Transformer Losses Due to Solar Penetration. *International Research Journal on Advanced Engineering and Management (IRJAEM)*, *2*(6), 1939–1945. https://doi.org/10.47392/irjaem.2024.0287

Shaoxin, M., Cihan, D., Zhiye, D., & Xue, C. (2019). Research on Transformer Flow-thermal Coupling Calculation Considering Harmonic Influence. *2019 IEEE International Conference on Power, Intelligent Computing and Systems (ICPICS)*, 397–401. https://doi.org/10.1109/ICPICS47731.2019.8942423

Si, W. R., Fu, C. Z., Wu, X. T., Zhou, X., Li, X. G., Yu, Y. T., Jia, X. Y., & Yang, J. (2020). Numerical Study of Electromagnetic Loss and Heat Transfer in an Oil-Immersed Transformer. *Mathematical Problems in Engineering*, *2020*. https://doi.org/10.1155/2020/6514650

Skillen, A., Revell, A., Iacovides, H., & Wu, W. (2012). Numerical prediction of local hot-spot phenomena in transformer windings. *Applied Thermal Engineering*, *36*(1), 96–105. https://doi.org/10.1016/j.applthermaleng.2011.11.054

Soleimani, M., & Kezunovic, M. (2021). Economic Analysis of Transformer Loss of Life Mitigation Using Energy Storage and PV Generation. *2020 IEEE/PES Transmission and Distribution Conference and Exposition (T&D)*. https://doi.org/10.1109/TD39804.2020.9299895

Soleimani, M., & Kezunovic, M. (2020). Mitigating Transformer Loss of Life and Reducing the Hazard of Failure by the Smart EV Charging. *IEEE Transactions on Industry Applications*, *56*(5), 5974–5983. https://doi.org/10.1109/TIA.2020.2986990

Taheri, A. A., Abdali, A., & Rabiee, A. (2019). A Novel Model for Thermal Behavior Prediction of Oil-Immersed Distribution Transformers with Consideration of Solar Radiation. *IEEE Transactions on Power Delivery*, *34*(4), 1634–1646. https://doi.org/10.1109/TPWRD.2019.2916664

Thango, B. A., & Bokoro, P. N. (2022). A Novel Approach to Predict Transformer Temperature Rise under Harmonic Load Current Conditions. *Energies*, *15*(8). https://doi.org/10.3390/en15082769

Thango, B. A., Sikhosana, L. S., Nnachi, A. F., & Jordaan, J. A. (2021). Loss financial evaluation and total ownership cost of transformers in large-scale solar plants. *2021 IEEE PES/IAS Power Africa*. https://doi.org/10.1109/PowerAfrica52236.2021.9543139

Uçar, B., Bağrıyanık, M., & Kömürgöz, G. (2017). Influence of PV Penetration on Distribution Transformer Aging. *Journal of Clean Energy Technologies*, *5*(2), 131–134. https://doi.org/10.18178/jocet.2017.5.2.357

Wan, D., Zhang, L., Zhao, M., & Zhou, H. (2019). Calculation Method of Hot Spot Temperature of Distribution Power Transmission Equipment Insulation Winding Based on Eddy Current Loss Density Distribution. *3rd IEEE Conference on Energy Internet and Energy System Integration*, 2750–2753. https://doi.org/10.1109/EI247390.2019.9062046

Xiao, D., Xiao, R., Yang, F., Chi, C., Hua, M., & Yang, C. (2022). Simulation research on onan transformer winding temperature field based on temperature rise test. *Thermal Science*, *26*(4), 3229–3240. https://doi.org/10.2298/TSCI211127047X

Yang, Z., Ruan, J., Huang, D., Du, Z., Tang, L., & Zhou, T. (2019). Calculation of Hot Spot Temperature of Transformer Bushing Considering Current Fluctuation. *IEEE Access*, *7*, 120441–120448. https://doi.org/10.1109/ACCESS.2019.2937510

Yuan, W., Yuan, X., Xu, L., Zhang, C., & Ma, X. (2023). Harmonic Loss Analysis of Low-Voltage Distribution Network Integrated with Distributed Photovoltaic. *Sustainability (Switzerland)*, *15*(5). https://doi.org/10.3390/su15054334